Modal Decoupling Control for Active Magnetic Bearing High-Speed Flywheel Rotor System with Strong Gyroscopic Effect

Changsheng Zhu*
College of Electrical Engineering
Zhejiang University, Hangzhou, China

Qi Zhang
College of Electrical Engineering
Zhejiang University, Hangzhou, China

Liangliang Chen
College of Electrical Engineering
Zhejiang University, Hangzhou, China

Abstract

In high-speed flywheel energy storage system, the high ratio of the polar to transverse mass moments of inertia of the flywheel rotor and the high operating speed have a great effect on the stability of the flywheel rotor system, traditional decentralized controllers, such as PID, are very difficult to deal with such rotor instability due to significant gyroscopic effect. In order to realize effectively the stability of active magnetic bearings(AMBs) supporting flywheel rotor system with strong gyroscopic effect at high rotating speeds, a new method called modal decoupling control is proposed in this paper based on mathematic model of the AMBs high-speed rigid flywheel rotor system. The principle of the modal decoupling control is introduced, and its ability and effectiveness to control the dynamic characteristics of the AMBs high-speed rigid flywheel rotor system are numerically analyzed and compared with the traditional PID controller. It is shown that the modal decoupling control proposed can separately regulate each mode' stiffness and damping through decoupling between the conical and the parallel modes, and obviously improve the dynamic behaviors and be capacity of stabilizing the AMBs high-speed rigid flywheel rotor system with strong gyroscopic effect in the high rotating speed region.

1 Introduction

In flywheel energy storage systems, a flywheel stores mechanical energy that interchanges in form of electrical energy by means of an electrical machine with a bidirectional power converter. The flywheel energy storage systems are suitable whenever numerous charge/discharge cycles (hundred of thousands) are needed with medium to high power (kW to MW) during short periods (seconds).

In order to maximize the energy density and the energy efficiency, the rotating speed of the flywheel should be as high as possible and the polar mass moment of inertia of the flywheel rotor should be as large as possible. Active magnetic bearings(AMB) is the best choose, in the support structure of a high speed flywheel energy storage system because of its no contact, no wear, no need of lubrication and dynamic adjustable. Therefore, the high-speed flywheel which is supported on magnetic bearings and made by composite materials is being considered as a promising and attracting one.

In the high-speed flywheel system, the high ratio of the polar to transverse mass moments of inertia of the flywheel rotor and the high rotating speed, the gyroscopic effect becomes more significant, which have a great effect on the stability of flywheel rotor system and greatly increase the complex of the control system, and may result in rotor instability in some cases. Traditional decentralized controllers, such as PID, are very difficult to deal with such instability due to significant gyroscopic effect[1-3]. In order to deal with such rotor instability, it is necessary to develop some advanced control methods.

In order to stabilize the high-speed flywheel system with strong gyroscopic effect, various control methods are presented. They are classified into two kinds, one is based on the modern control, such as sliding mode controller[4,5], μ synthesis controller[6,7], robust gain-scheduled H_∞ controller[8.9], LQR controller[10,11], These control can get a

*E-mail: cszhu@hotmail.com, Phone Number:0086-571-87983515, Fax Number:0086-571-87951625

good performance, but it is difficult to realize due to more large time-consuming. The other is based on the traditional decentralized controller with cross-feedback[12-15], which has a simple structure and good performance, but designing a good control is not so easily due to the couple between different modes.

A new method called modal decoupling control is proposed in this paper based on mathematic model of the AMBs high-speed rigid flywheel rotor system. The principle of the modal decoupling control is introduced, and its ability and effectiveness to control the dynamic characteristics of the AMBs high-speed rigid flywheel rotor system are numerically analyzed and compared with the traditional PID controller and the cross-feedback controller. It is shown that the modal decoupling control proposed can separately regulate each mode' stiffness and damping of the AMBs high-speed rigid flywheel rotor system through decoupling between the conical and the parallel modes, and obviously improve the dynamic behaviors and be capacity of stabilizing the AMBs high-speed rigid flywheel rotor system with strong gyroscopic effect in the high rotating speed region.

2 Model of the AMBs-Rigid Flywheel Rotor System

In the most high-speed flywheel energy storage systems, the bending critical speed of the flywheel rotor system is much more than the operating speed, so the flywheel rotor system is often considered as a rigid shaft. Figure 1 shows the schemical of a simplified model of the vertically rigid flywheel rotor system supported by a pair of permanent material(PM) bearings located on the top and bottom sides and radically by two AMBs, the rotor positions are measured by four eddy current-type sensors.

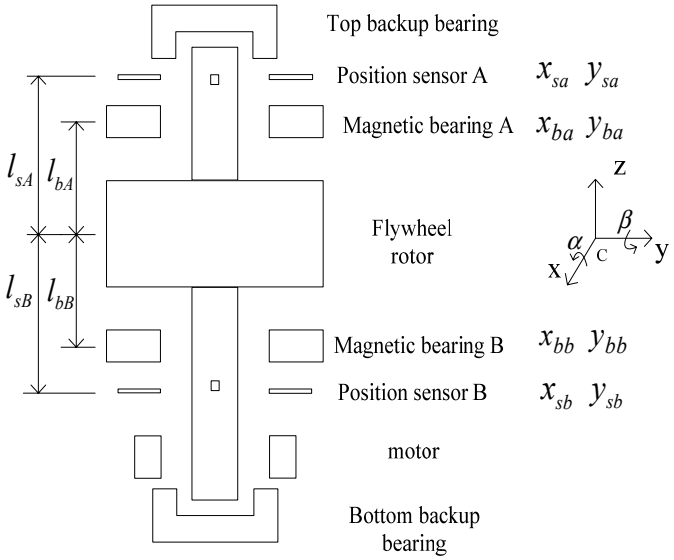

Figure1: Schemical of the AMBs rigid flywheel rotor system

In order to describe the motions of the flywheel rotor system, it is assumed that the axial line of the rotor is centralized as the geometric centers of two radial AMBs. Three coordinate systems are defined, which are sensor coordinate systems $o_{sA}x_{sA}y_{sA}$ and $o_{sB}x_{sB}y_{sB}$, radial AMB coordinate systems $o_{bA}x_{bA}y_{bA}$ and $o_{bB}x_{bB}y_{bB}$ and rotor coordinate system *oxyz*, respectively. All original points of coordinate systems are the geometric centre of two radial AMBs. The rotor coordinate system *oxyz* is fixed to the mass center of flywheel rotor system and *z* axis to the spinning axis of the flywheel rotor system. The *x* and *y* denote the linear displacements of the mass center of flywheel rotor along the *x* and *y* axes, respectively, and θ_x and θ_y the angular displacements of flywheel rotor about the *x* and *y* axes. The coordinates of the rotor at the upper sensor and the lower sensor positions are (x_{sA} , y_{sA}) and (x_{sB} , y_{sB}). The coordinates of the rotor at the upper radial AMB and the lower radial AMB positions are (x_{bA} , y_{bA}) and (x_{bB} , y_{bB}). The relative positions between the sensors, radial AMBs and mass center of flywheel rotor system are also shown in Figure 1.

In order to simplify theoretical analysis, the following assumptions are made: a) coupling between the axial PM bearings and the radial AMBs is neglect; b) radial AMBs are symmetrical in geometry for the *x* and *y* axes and coils parameters in every polar are same; c) no coupling effect between magnetic poles in the radial AMBs; d) radial AMBs are isotropic and the AMBs magnetic forces are simplified by a linear model.

For the motion of the rotor in the radial directions, the equations of motion of flywheel rotor system in x, y, θ_x and θ_y are

$$\begin{cases} m\ddot{x} = f_{xA} + f_{xB} + u_x \\ m\ddot{y} = f_{yA} + f_{yB} + u_y \\ J_x\ddot{\theta}_y - J_z\omega\dot{\theta}_x = f_{xA}l_{Ba} - f_{xB}l_{Bb} \\ J_y\ddot{\theta}_x + J_z\omega\dot{\theta}_y = -f_{yA}l_{Ba} + f_{yB}l_{Bb} \end{cases} \tag{1}$$

where m is the total mass of the flywheel rotor, $J_x = J_y = J$ are transverse mass moments of inertia of the flywheel rotor around *x* and *y* axis, J_z is polar mass moment of inertia of the spinning flywheel rotor around *z* axis, ω is rotating speed about the spinning axis *z*. u_x and u_y are components of the rotor imbalance force in the *x* and *y* directions. f_{xA}, f_{yA}, f_{xB} and f_{yB} are magnetic forces acting on the flywheel rotor in the lower and the upper radial AMBs, which are

$$\begin{cases} f_{xA} = k_{sA}x_{bA} + k_{iA}i_{xA} \\ f_{xB} = k_{sB}x_{bB} + k_{iB}i_{xB} \\ f_{yA} = k_{sA}y_{bA} + k_{iA}i_{yA} \\ f_{yB} = k_{sB}y_{bB} + k_{iB}i_{yB} \end{cases} \tag{2}$$

where (k_{sA} k_{iA}) and (k_{sB} k_{iB}) are force-displacement and force-current coefficients of the upper and the lower radial AMBs, respectively. (i_{xA} i_{yA}) and (i_{xB} i_{yB}) are control currents of the upper and the lower radial AMBs, respectively.

The matrix form of the magnetic forces acting on the flywheel rotor can be expressed as

$$f = K_S q_b + K_i i \tag{3}$$

where $f = \{f_{xA}\ f_{xB}\ f_{yA}\ f_{yB}\}^{\mathrm{T}}$ is the magnetic force vector acting on the flywheel rotor, K_S and K_i are the force-displacement matrix and force-current matrix of the ABMs, respectively. $i = [i_{xA}\ i_{xB}\ i_{yA}\ i_{yB}]^{\mathrm{T}}$ is control current. $q_b = \{x_{bA}\ x_{bB}\ y_{bA}\ y_{bB}\}^{\mathrm{T}}$ is the generalized coordinate vector at the two radial AMBs. $K_S = \begin{bmatrix} K_{S11} & 0 \\ 0 & K_{S22} \end{bmatrix}$, $K_{S11} = \begin{bmatrix} k_{sA} & 0 \\ 0 & k_{sA} \end{bmatrix}$, $K_{S22} = \begin{bmatrix} k_{sB} & 0 \\ 0 & k_{sB} \end{bmatrix}$, $K_i = \begin{bmatrix} K_{i11} & 0 \\ 0 & K_{i22} \end{bmatrix}$, $K_{i11} = \begin{bmatrix} k_{iA} & 0 \\ 0 & k_{iA} \end{bmatrix}$, $K_{i22} = \begin{bmatrix} k_{iB} & 0 \\ 0 & k_{iB} \end{bmatrix}$.

In Equation (2), (x_{bA}, y_{bA}) and (x_{bB}, y_{bB}) are the rotor coordinates at the upper and the lower radial AMBs, the transform relation between the rotor coordinates at the upper and the lower radial AMBs and the mass centre coordinates of the flywheel rotor system, x, y, θ_x and θ_y is

$$q_b = \begin{Bmatrix} x_{bA} \\ x_{bB} \\ y_{bA} \\ y_{bB} \end{Bmatrix} = \begin{bmatrix} l_{bA} & 1 & 0 & 0 \\ l_{bB} & 1 & 0 & 0 \\ 0 & 0 & -l_{bA} & 1 \\ 0 & 0 & -l_{bB} & 1 \end{bmatrix} \begin{Bmatrix} \theta_y \\ x \\ \theta_x \\ y \end{Bmatrix} = T_b q \tag{4}$$

Finally, the matrix form of the equations of motion of rigid flywheel rotor system is

$$M\ddot{q} + G\dot{q} - K_{ss}q = LK_i i + U \tag{5}$$

where $q=\{\theta_y \;\; x \;\; \theta_x \;\; y\}^{\mathrm{T}}$, $M=\begin{bmatrix} m_J & 0 \\ 0 & m_J \end{bmatrix}$, $m_J=\begin{bmatrix} J & 0 \\ 0 & m \end{bmatrix}$, $G=\begin{bmatrix} 0 & -J_\Omega \\ J_\Omega & 0 \end{bmatrix}$, $J_\Omega=\begin{bmatrix} J_z\omega & 0 \\ 0 & 0 \end{bmatrix}$, $L=\begin{bmatrix} l_{b11} & 0 \\ 0 & l_{b22} \end{bmatrix}$, $l_{b11}=\begin{bmatrix} l_{bA} & -l_{bB} \\ 1 & 1 \end{bmatrix}$, $l_{b22}=\begin{bmatrix} -l_{bA} & l_{bB} \\ 1 & 1 \end{bmatrix}$, $K_{\mathrm{ss}}=LK_sL^{\mathrm{T}}$, $U=\{0 \;\; u_x \;\; 0 \;\; u_y\}^{\mathrm{T}}$ is rotor unbalance force vector.

The transform function block of the flywheel rotor system based on the equations of motion of flywheel rotor system is shown in Figure 2. It is shown that the coupling between θ_x and θ_y is greatly depend on the ratio of the polar to transverse mass moments of inertia of the flywheel rotor and the rotating speed of the flywheel rotor.

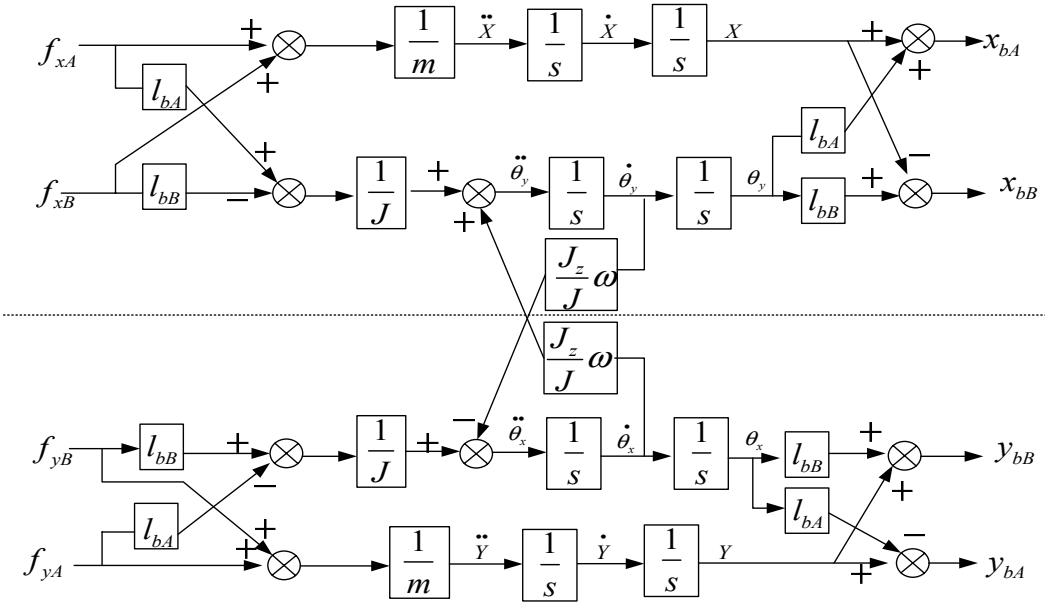

Figure 2: Transform function block diagram of the flywheel rotor system

For the decentralized PD controller, let its output current be

$$i=-Pq_b-D\dot{q}_b \tag{6}$$

where $q_b=\{x_{bA} \;\; x_{bB} \;\; y_{bA} \;\; y_{bB}\}$ is the generalized coordinate vector of two radial AMBs positions. $P=diag\left(p_{xA} \;\; p_{xB} \;\; p_{yA} \;\; p_{yB}\right)$ is the proportional gain coefficient matrix, $D=diag\left(d_{xA} \;\; d_{xB} \;\; d_{yA} \;\; d_{yB}\right)$ is the differential gain coefficient matrix. When the AMBs are symmetrical, the proportional and the differential gain coefficients are same for every channel at the upper and the lower radial AMBs, i.e., $p_{xA}=p_{yA}=p_A$, $p_{xB}=p_{yB}=p_B$, $d_{xA}=d_{yA}=d_A$, $d_{xB}=d_{yB}=d_B$.

Submitting Equation (6) to Equation (5), we have

$$M\ddot{q}+G\dot{q}-K_{ss}q=-L_fK_i(Pq_b+D\dot{q}_b) \tag{7}$$

Since $q_b=L_f^Tq$, so

$$M\ddot{q}+G\dot{q}-K_{ss}q+L_fK_iPL_f^Tq+L_fK_iDL_f^T\dot{q}=0 \tag{8}$$

Let $K_c=L_fK_iPL_f^T$, $D_c=L_fK_iDL_f^T$, we have

$$M\ddot{q}+(G+D_c)\dot{q}+(-K_{ss}+K_c)q=0 \tag{9}$$

where $K_c = \begin{bmatrix} K_{C11} & 0 \\ 0 & K_{C22} \end{bmatrix}$, $K_{C11} = \begin{bmatrix} k_{iA}p_A(l_{bA}^2 + l_{bB}^2) & k_{iA}p_A(l_{bA} - l_{bB}) \\ k_{iA}p_A(l_{bA} - l_{bB}) & 2k_{iA}p_A \end{bmatrix}$, $K_{C22} = \begin{bmatrix} k_{iB}p_B(l_{bA}^2 + l_{bB}^2) & k_{iB}p_B(-l_{bA} + l_{bB}) \\ k_{iB}p_B(-l_{bA} + l_{bB}) & 2k_{iB}p_B \end{bmatrix}$,

$D_c = \begin{bmatrix} D_{C11} & 0 \\ 0 & D_{C22} \end{bmatrix}$, $D_{C11} = \begin{bmatrix} k_{iA}d_A(l_{bA}^2 + l_{bB}^2) & k_{iA}d_A(l_{bA} - l_{bB}) \\ k_{iA}d_A(l_{bA} - l_{bB}) & 2k_{iA}d_A \end{bmatrix}$, $D_{C22} = \begin{bmatrix} k_{iB}d_B(l_{bA}^2 + l_{bB}^2) & k_{iB}d_B(-l_{bA} + l_{bB}) \\ k_{iB}d_B(-l_{bA} + l_{bB}) & 2k_{iB}d_B \end{bmatrix}$.

It is shown that K_c and D_c can be considered as the stiffness and damping proved by the PD controller. In order to make all polar points in the close system be in the negative half-plane, i.e., in order to stabilize the rotor system, K_c should be larger enough to compensate the negative stiffness matrix K_{ss}. The damping matrix D_c should be positive in order to make the system be asymptotically stable, i.e., all eigenvalues of the close-loop system are in the negative half-plane.

3 Principle of Modal Decoupling Control

The purpose of the modal decoupling control is to separately regulate each mode's stiffness and damping of the flywheel rotor system through decoupling between conical and parallel modes. Therefore, the first is to cancel the effect of the negative stiffness of AMBs by adding an equal and opposite stiffness to the current command signal in order to make the flywheel rotor become a free rotor to which the modal decoupling control can be applied. The second, an input transformation matrix T_{in} is added at the input side of the controller to convert the sensor displacements, x_{sA}, y_{sA}, x_{sB} and y_{sB}, to the displacements of mass center of the flywheel rotor system x, y, θ_x and θ_y. The third, an output transformation matrix T_{out} is added at the output side of the controller to convert the current command signals about the mass center displacements x, y, θ_x and θ_y to the current commands about the AMBs displacements x_{bA}, x_{bB}, y_{bA} and y_{bB}. The block diagram of modal decoupling controller is shown in Figure 3.

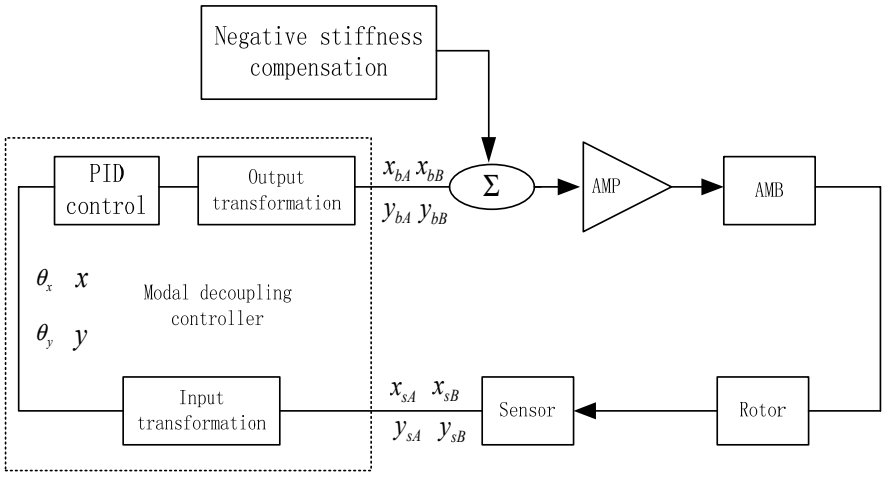

Figure 3: Block diagram of modal decoupling control

From Equation (5), it is found that when $l_{bA} \neq l_{bB}$, i.e., the distance between the upper AMB to the mass center of flywheel rotor system is not the same as that between the lower to the mass center of flywheel rotor system, the negative stiffness matrix K_{ss} is not diagonal, the decoupling effect will be weaken. It also means that when there is a displacement in the mass centre of flywheel rotor, the magnetic forces produced by the upper and lower AMBs are same for $l_{bA} = l_{bB}$, but different for $l_{bA} \neq l_{bB}$. The different magnetic forces will result in a moment in the flywheel rotor about the mass center of the flywheel rotor which will make the rotor tile. On the other hand, in order to directly apply the proportional and the differential parameters of the PD control to rotor modes, it is necessary to compensate the negative stiffness matrix K_{ss}.

It is assumed that the control current for the power amplifier, *i*, is decomposed into a modal decoupling current i_c and a negative stiffness compensation current i_k i.e.

$$i = i_c + i_k \tag{10}$$

Submitting Equation (10) to Equation (5), we have

$$M\ddot{q} + G\dot{q} - K_{ss}q = L_f K_i i_c + L_f K_i i_k + U \tag{11}$$

In order to completely compensate the negative stiffness, the following relation must be satisfied.

$$K_{ss}q + L_f K_i i_k = 0 \tag{12}$$

Using the transform relation between the AMBs coordinates and the mass centre coordinates of the flywheel rotor system, $q_b = T_b q$ we have the compensation current i_k

$$i_k = -K_i^{-1} L_f^{-1} K_{ss} T_b^{-1} q_b \tag{13}$$

Let $T_{ss} = K_i^{-1} L_f^{-1} K_{ss}$, therefore

$$T_{ss} = \frac{k_s}{k_i(l_{bA}+l_{bB})}\begin{bmatrix} l_{bA}^{\ 2}+l_{bA}l_{bB} & l_{bA}+l_{bB} & 0 & 0 \\ -l_{bA}l_{bB}-l_{bB}^2 & l_{bA}+l_{bB} & 0 & 0 \\ 0 & 0 & -l_{bA}^{\ 2}-l_{bA}l_{bB} & l_{bA}+l_{bB} \\ 0 & 0 & l_{bA}l_{bB}+l_{bB}^2 & l_{bA}+l_{bB} \end{bmatrix} \tag{14}$$

For the decentralized PD controller, let the modal decoupling control i_c be

$$i_c = -Pq_s - D\dot{q}_s \tag{15}$$

where $P = diag\left(p_{xA}\ \ p_{xB}\ \ p_{yA}\ \ p_{yB}\right)$ is the proportional gain coefficient matrix, $D = diag\left(d_{xA}\ \ d_{xB}\ \ d_{yA}\ \ d_{yB}\right)$ is the differential gain coefficient matrix.

The input of the decentralized PD controller is the signals from the sensors, i.e., x_{sA}, x_{sB}, y_{sA} and y_{sB}, the relation between the sensor signals and the coordinates of the rotor mass center, x, y, θ_x and θ_y, is

$$\begin{cases} x = \dfrac{l_{sB}}{l_{sA}+l_{sB}}x_{sA} + \dfrac{l_{sA}}{l_{sA}+l_{sB}}x_{sB} \\ y = \dfrac{l_{sB}}{l_{sA}+l_{sB}}y_{sA} + \dfrac{l_{sA}}{l_{sA}+l_{sB}}y_{sB} \\ \theta_x = \dfrac{y_{sA}-y_{sB}}{l_{sA}+l_{sB}} \\ \theta_y = \dfrac{x_{sB}-x_{sA}}{l_{sA}+l_{sB}} \end{cases} \tag{16}$$

It is shown that the input variation in any controller's channel will result in the change of both linear and angle displacements of the rotor mass center. It means that the conical mode and the parallel mode are coupled each other. Therefore, the sensor coordinates x_{sA}, x_{sB}, y_{sA} and y_{sB} should transform to the rotor mass centre coordinates x, y θ_x and θ_y. Using the relation between q_b and q, $q = T_b^{-1} q_s$, i.e., a relation matrix between the sensors and the PD controller $T_{in} = T_b^{-1}$ adds in order to directly control the signals of the every modal coordinates, so

$$T_{in} = T_b^{-1} = \begin{bmatrix} \frac{1}{l_{sA}+l_{sB}} & \frac{-1}{l_{sA}+l_{sB}} & 0 & 0 \\ \frac{l_{sB}}{l_{sA}+l_{sB}} & \frac{l_{sA}}{l_{sA}+l_{sB}} & 0 & 0 \\ 0 & 0 & \frac{-1}{l_{sA}+l_{sB}} & \frac{1}{l_{sA}+l_{sB}} \\ 0 & 0 & \frac{l_{sB}}{l_{sA}+l_{sB}} & \frac{l_{sA}}{l_{sA}+l_{sB}} \end{bmatrix} \tag{17}$$

It is clear that since the matrix $L_f K_i$ is not a diagonal matrix, so there is a coupling between the conical mode and the parallel mode. In order to decouple between the conical mode and the parallel mode in the output, it is necessary to add an output transformation matrix T_{out} to make the matrix $L_f K_i T_{out}$ be a diagonal one. There are many choose for making the matrix $L_f K_i T_{out}$ be a diagonal matrix, it is chosen $L_f K_i T_{out} = I$ in this paper, so

$$T_{out} = K_i^{-1} L_f^{-1} = \frac{1}{k_i(l_{sA}+l_{sB})} \begin{bmatrix} 1 & l_{sB} & 0 & 0 \\ -1 & l_{sA} & 0 & 0 \\ 0 & 0 & -1 & l_{sB} \\ 0 & 0 & 1 & l_{sA} \end{bmatrix} \tag{18}$$

After the decoupling in the input side, the controller can directly adjust the any mode of the flywheel rotor system. In this case, the input signals of the control are the mass centre coordinates, not the signals of the sensors. Since the control forces are only provided by the AMBs, the moment signals must be transferred to the AMBs force signals, in order to decouple the input and output of the controller, the currents of the PD controller are

$$i_c = -K_i^{-1} L_f^{-1} (P + D) T_b^{-1} q_b \tag{19}$$

Finally, the control currents of the modal decoupling control strategy is

$$i = i_c + i_k = -K_i^{-1} L_f^{-1} (P + D + K_{ss}) T_b^{-1} q_b = -T_{out} (P + D + K_{ss}) T_{in} q_b \tag{20}$$

With the modal decoupling control, the equations of motion of the flywheel rotor system are:

$$M\ddot{q} + G\dot{q} + Pq + D\dot{q} = U \tag{21}$$

$$P = diag(p_r, p_p, p_r, p_p) \tag{22}$$

$$D = diag(d_r, d_p, d_r, d_p) \tag{23}$$

where p_r, d_r, p_p and d_p are proportional and differential coefficients of the modal decoupling control for conical mode and parallel mode, respectively. The negative stiffness compensation signal is $K_i^{-1} L^{-1} k_{ss} L_s^{-1} q_s$.

From Equations (21)-(23), it is found that the conical mode and the parallel mode are independent, so stiffness and damping of the conical mode and the parallel mode can be separately controlled by varying the controller's parameters p_r, d_r, p_p or d_p. On the other hand, the gyroscope matrix of the flywheel rotor system only affects the conical mode and does not affect the parallel mode, so the gyroscope effect on the flywheel rotor modes significantly decreases.

4 Numerical Results and Analysis

The basic parameters of the symmetrically rigid flywheel rotor supported on AMBs are: total mass of the flywheel rotor m=25.8 kg, distances between the rotor mass center and two radial AMBs center l_{bA}=200 mm and l_{bB}=-200 mm distance between the rotor mass center and two sensor centers l_{sA}=250 mm and l_{sB}=-250 mm, transverse mass moment of inertia of the flywheel rotor system around the x and y axes J_x =J_y =0.1151 kgm^2, polar mass moment of

inertia of the flywheel rotor system around the z axis J_z=0.2388 kgm^2, radial clearance of the two radial AMBs C_o=0.4 mm, current stiffness coefficients of the two radial AMBs $k_i = 37.7$ N/A , displacement stiffness coefficients of the two radial AMBs $k_x = -15.08\times10^4$ N/m , mass eccentricity of the flywheel rotor $e_\mu = 1\times10^{-6}$ m.

4.1 Modes Analysis

Figure 4 shows that the mode frequencies of the rigid flywheel rotor system with the rotating speed ω. The thick solid line is the synchronous speed. The flywheel rotor system both in no-rotating and rotating cases has two kinds of natural rigid body mode, i.e., conical mode and the parallel mode. The conical mode describes rotor tilt around its center of mass. The parallel mode describes the motion of the rotor mass center in xy plane, no any tilting in the flywheel rotor. When the rotor is spinning, the parallel mode frequency does not change any more with the rotating speed, it means the gyroscope effect does not affect the parallel mode, but the conical mode separates with the increase of rotating speed into nutation mode and precession mode. The nutation mode rotates in the same direction as rotor rotation, and precession mode in the opposite direction as rotor rotation. The nutation mode frequency increases with the rotating speed, but the precession mode frequency decreases.

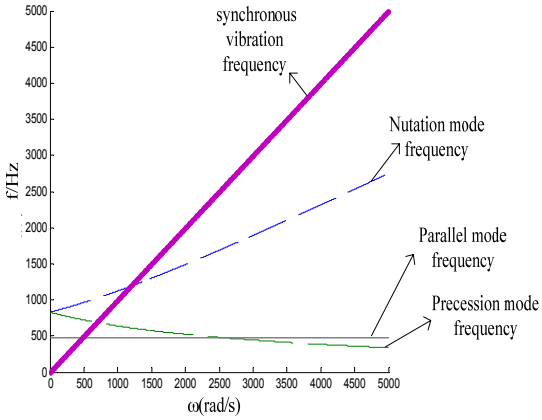

Figure 4: Rigid body mode frequencies with rotational speeds

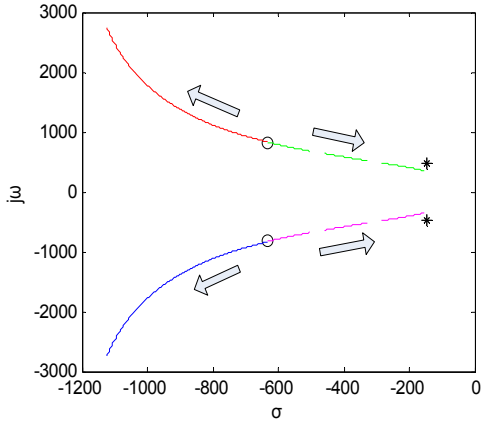

Figure 5: Variation of eigenvalues of the flywheel rotor with the rotating speeds

The variation of the eigenvalues of the flywheel rotor system with the rotating speed is shown in Figure 5, where σ and $j\omega$ are the real and imaginary parts of the eigenvalue, respectively. The real part of the eigenvalue stands for the stability of the flywheel rotor system, and the imaginary part for the vibration frequency. The eigenvalues of the flywheel rotor system without rotating are shown by two circles for conical modes and two stars for the parallel modes. The real part of the precession mode in solid line increases with the rotating speed, but the real part of the nutation mode in dashed line decreases with the rotating speed. The real part and imaginary part of the parallel modes does not change any more with the increase of the rotating speed. In the high rotating speeds, the precession mode with a very high frequency is very difficult to control and may result in the system instability due to the time delay in the control system and limited bandwidths of power amplifiers and sensors. Both the real part and the imaginary part of the nutation mode are approach to zero, the stability of the flywheel rotor system becomes very weak, and may also result in rotor instability due to small damping and phase leg in the control system. Therefore, the stability of the flywheel rotor system is mainly determined by the conical modes. It is necessary to regulate the conical mode and the parallel mode frequency independently.

The variation of mode frequencies of the flywheel rotor system with the decentralized PD controller with the proportional factor P at 0 rpm is shown in Figure 6. It is shown that both the conical mode frequency in solid line and the parallel mode frequency in dish line increase when the proportional factor P increases. Even when the conical mode frequency is close to zero, the parallel mode frequency is about 150 Hz. In such high frequency, it is difficult to get an appropriate mode frequency to improve system stability. Therefore, the decentralized PD controller can not separately regulate each mode's stiffness and damping of the flywheel rotor system.

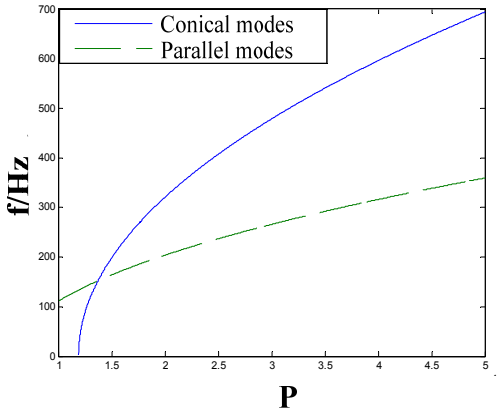

Figure 6: Mode frequencies variation with P at the decentralized PD controller

The variations of the conical and the parallel mode frequencies along with the proportional factor of the conical mode control channel p_r and the proportional factor of the parallel mode control channel p_p is shown in Figures 7 and 8, respectively. It is shown that the conical mode frequency goes up as the proportional factor of the conical mode control channel p_r increases, whereas the parallel mode frequency always remains constant. Similarly, the parallel modes frequency goes up as the proportional factor of the parallel modes control channel p_p increases, whereas the conical modes frequency still remains constant. Hence, the parallel modes control channel and the conical modes control channel are totally independent, which allow us to regulate the different modes' stiffness through changing the proportional factor of the corresponding mode control channel.

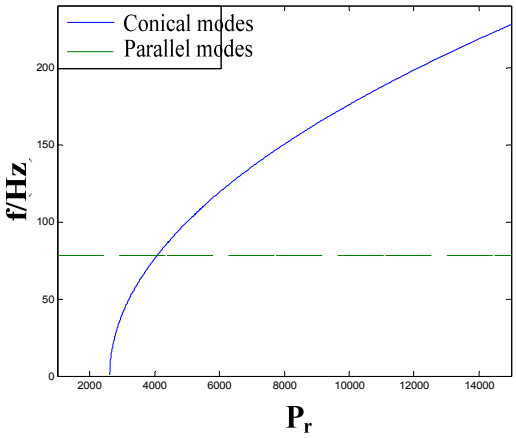

Figure 7: Mode frequencies variation with p_r at modal decoupling control

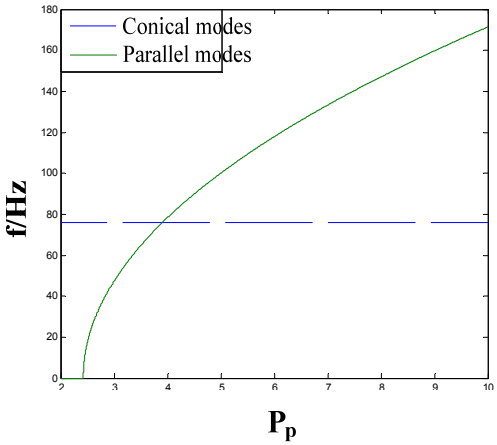

Figure 8: mode frequencies variation with p_p at modal decoupling control

4.2 Rotor Motion Control

The simulation result of motion track of the AMBs high-speed rigid flywheel rotor system with a suitable decentralized PD controller at 60000 rpm is shown in Figures 9 and 10. In the simulation, the initial positions of the rotor system in sensors center are $[x_{sA}\ x_{sB}\ y_{sA}\ y_{sB}] = [-0.025\ \ 0.2\ \ 0.025\ \ 0.2]$ mm. It is shown that in this rotational speed, the rotor system with decentralized PD controller is stable, but the vibration decay is much slow. In practice, the rotor very easily loses it stability due to large time delay in the control system.

Simulation results of motion track of the AMBs high-speed rigid flywheel rotor system with the modal decoupling control at the same initial positions as in Figure 9 and 10 are shown in Figures 11 and 12, it is shown that

the rotor vibration decay is much fast and the modal decoupling control is an effective way to constrain the gyroscopic effect of flywheel rotor and improve the stabilization of the AMBs flywheel rotor system.

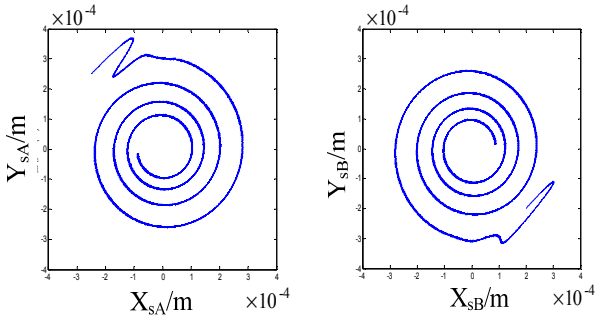

(a) Motion track of A plane (b) Motion track of B plane

Figure 9: Motion track of flywheel rotor with decentralized PD controller

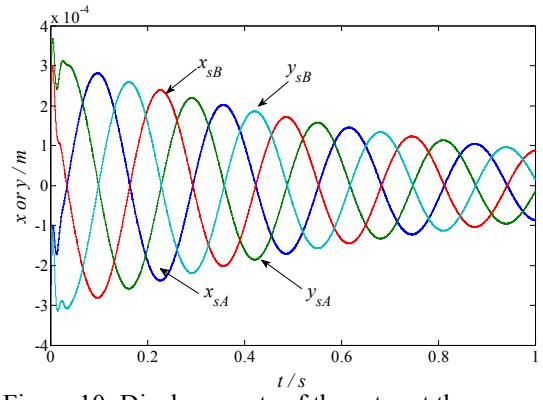

Figure 10: Displacements of the rotor at the sensor locations with decentralized PD controller

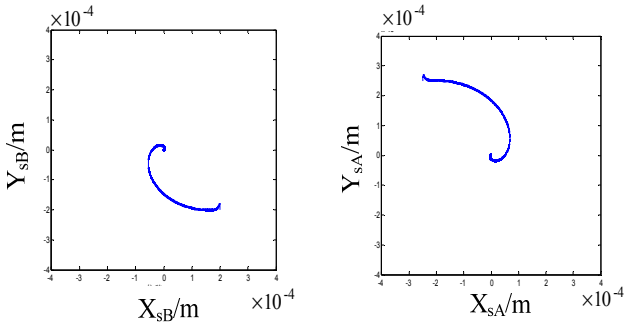

(a) Motion track of A plane (b) Motion track of B plane

Figure 11: Motion track of flywheel rotor with modal decoupling control

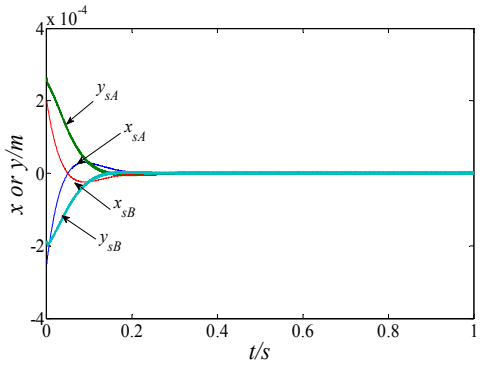

Figure 12: Displacements of the rotor at the sensor locations with modal decoupling control

In order to show the robust performance of the modal decoupling control for the disturbance, a step position disturbance is applied on the *x* direction of the upper sensor at the time of 0.4s and final displacement of 0.25mm. Since there is integration part in both decentralized PD controller and modal decoupling control, the final position of the *x* direction of the upper sensor should be at the position of (-0.25 0) mm. The simulation results of motion track of the flywheel rotor system with decentralized PD controller at 60000 rpm after a step position disturbance are shown in Figures 13 and 14. It is also shown that for the decentralized PD controller, the final position is same, but it takes a long time, and the rotor vibrations are large.

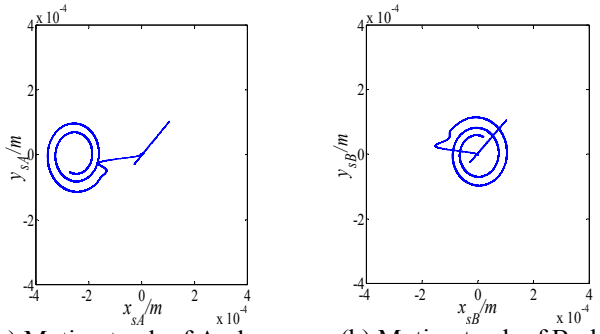

(a) Motion track of A plane (b) Motion track of B plane

Figure 13: Motion track of flywheel rotor with decentralized PD controller after a step disturbance

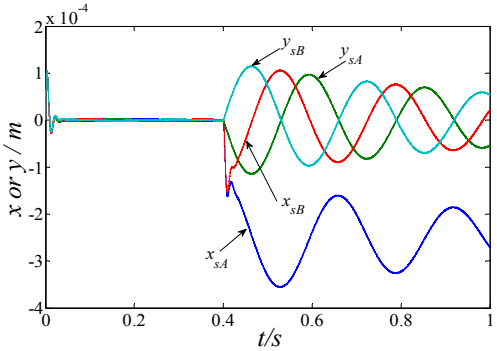

Figure 14: Displacements of the rotor at the sensor locations with decentralized PD controller after a step disturbance

The simulation results of motion track of the flywheel rotor system with modal decoupling control at the same conditions are shown in Figures 15 and 16. It is also show that for the decentralized PD controller, it takes a very short time to final position and the rotor vibrations are very small. Therefore, the modal decoupling control has more robust performance for the disturbance.

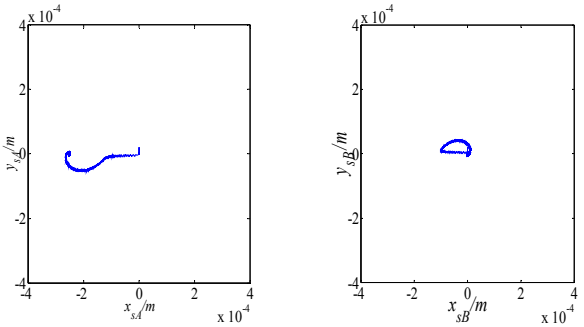

(a) Motion track of A plane (b) Motion track of B plane

Figure 15: Motion track of flywheel rotor with modal decoupling control after a step disturbance

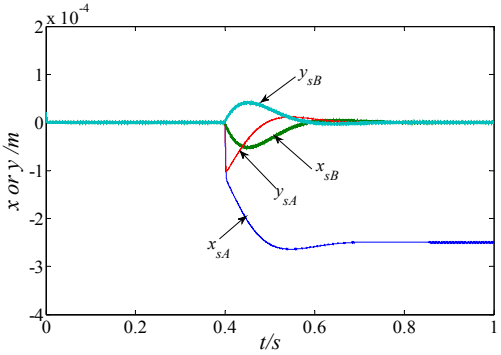

Figure 15: Displacements of the rotor at the sensor locations with modal decoupling control after a step disturbance

5 Conclusion

A new method called modal decoupling control is proposed in this paper based on mathematic models of the flywheel rotor system. It is shown that the modal decoupling control can separately regulate each mode's stiffness and damping of the AMBs high-speed flywheel rotor system through decoupling between the conical mode and the parallel mode, and obviously improve the dynamic behaviors and be capacity of anti-interference of the AMBs high-speed flywheel rotor system with strong gyroscopic effect.

References

[1] Ahrens M, Kucera L. Performance of a magnetically suspended flywheel energy storage device. IEEE Transaction on Control Systems Technology, 1996, 4(5):494-502

[2] Hannes B. Decentralized control of magnetic rotor bearing systems. Federal Institute of Technology (ETH), Zurich, Switzerland, 1984.

[3] Kascak A F. Stability limits of a PD controller for a flywheel supported on rigid rotor and magnetic bearings. Proceedings of Navigation and Controls Conference. San Francisco, 2005, pp:2005-5956.

[4] Sivrioglu S, Nonami K. Sliding mode control with time-varying hyperplane for AMB systems. IEEE/ASME Transaction on Mechatronics, 1998, 3(1):51-59.

[5] Ann R, Raymond D. A sliding mode observer and controller for stabilization of rotational motion of a vertical shaft magnetic bearing. IEEE Transactions on Control Systems Technology, 1996, 4(5):598-608.

[6] Nonami K, Ito T. μ synthesis of flexible rotor-magnetic bearing systems. IEEE Transactions on Control Systems Technology, 1996, 4(5):503-512.

[7] Schönhoff U, Luo J, Li G, et al. Implementation results of μ-synthesis control for an energy storage flywheel test rig. Proceedings of the 7th International Symposium on Magnetic Bearings. Switzerland, 2000, pp:317-322.

[8] Sivrioglu S, Nonami K. LMI approach to gain scheduled H_∞ control beyond *PID* control for gyroscopic rotor-magnetic bearing system. Proceedings of the 35th Conference on Decision and Control, Japan, 1996, 6:3694-3699.

[9] Herzog R. Ein beitrag zru regelung von magnetgelagerten Systemenmittels positive reeller funktionen und H infinity-optimierung. Switzerland, Swiss Federal Institute of Technology, 1998.

[10] Efrain P, Douglas B, Edson K. Vibration control using active magnetic actuators with the LQR control technique. Proceedings of the 7th Brazilian Conference on Dynamics, Control and Applications. Brazil, 2008, pp:1-6.

[11] Zhu KY, Xiao Y, Acharya U. Rajendra. Optimal control of the magnetic bearings for a flywheel energy storage system. Mechatronics, 2009, 19(8):1221-1235
[12] Gerald V B. Stability gyroscopic modes in magnetic bearing supported flywheels by using cross-axis proportional gains. Proceedings of Navigation and Controls Conference. San Francisco, 2005, pp:2005-5955.
[13] Ahrens M, Kucera L. Cross feedback control of a magnetic bearing system controller design considering gyroscopic effects. Proceedings of 3rd International Symposium on Magnetic Suspension Technology, ETH, 1996, pp:177-191.
[14] Zhao L, Zhang K, Zhu R S, et al. Experimental research on a momentum wheel suspended by active magnetic bearings. Proceedings of the 8th International Symposium on Magnetic Bearings, University of Ibaraki, 2002, pp:605-609.
[15] Okada Y, Nagai B. Cross-feedback stabilization of the digitally controlled magnetic bearing. Journal of Vibration, Acoustics, Stress, and Reliability in Design, 1992, 114(1):54-59

Acknowledgement

The research was supported by Commonweal Technology Application Research Project of Department of Science and Technology of Zhejiang Province(2011C21021) and National High Technology Research and Development Program of China(2006AA05Z201).